Materials Transactions, Vol. 44, No. 9 (2003) pp. 1802 to 1808

Strain Enhanced Growth of Precipitates during Creep of T91

Takeshi Nakajima[1,*], Stefano Spigarelli[2], Enrico Evangelista[2] and Takao Endo[1]

[1]*Department of Materials Engineering, Yokohama National University, Yokohama 240-8501, Japan*
[2]*Department of Mechanics, University of Ancona, Via Brecce Bianchi 1-60131, Ancona, Italy*

The previous work showed that the precipitate coarsening of T91 (Modified 9Cr–1Mo steel) was described by an empirical relationship depending on applied stress. However, there is another possibility that the stress dependent coarsening is merely apparent and strain dependent actually. In the present paper, an attempt was made to re-analyze the previous data based on a model in which the effective diffusivity of solute is strain dependent. The result of analysis suggests strongly that the dislocation dragging solute atmosphere causes the enhancement of solute diffusivity and leads to the promoted growth of precipitates.

(Received June 3, 2003; Accepted July 22, 2003)

Keywords: *T91, creep, precipitate, Ostwald ripening, diffusion, atmosphere*

1. Introduction

Mod.9Cr–1Mo steel (T91) is one of the ferritic heat resistant steels used widely for fossil power plants because of its excellent high temperature strength and the advantage of small thermal stress in cyclic operations. After a conventional heat treatment, *i.e.*, normalizing and tempering, the transformed microstructure exhibits elongated fine subgrains that evolve during creep into coarse and equi-axed ones. It has densely populated dislocations while free dislocation density decreases gradually.[1–7] Since the deterioration of creep strength is accompanied by the loss of dislocation density and subgrain coarsening, the thermal stability of microstructure is of vital importance for heat resistant steels.[6–9]

The microstructural stability of ferritic heat resistant steels is mainly controlled by the thermal stability of precipitates that are able to retard the growth rate of subgrains.[10] In the case of T91, two kinds of precipitates, $M_{23}C_6$ and MX, contribute to the structural stability, and they also act as the origin of threshold stress for creep.[11–13]

Two of the present authors (Spigarelli and Evangelista) have studied the coarsening law of T91 to understand the difference in creep behavior of some ferritic steels.[13] They obtained the empirical coarsening law exhibiting apparent stress dependence. Using this empirical relationship they explained the creep behavior of some ferritic steels successfully on the basis of threshold concept.[13] However, there is another possibility that the applied stress dependence of coarsening is merely apparent and strain dependent actually. In practice, some investigators have suggested the possibility that the precipitate coarsening was promoted by creep strain.[14,15] In the present paper, the previous data[13] along with some added ones will be re-analyzed using a simple model in which effective diffusivity is strain dependent.

2. Growth of Precipitate

Structural stability of advanced heat resistant steels relies on the phase stability, growth of precipitates, nucleation of new phases and so on. Among these factors, coarsening of precipitates is one of the most important deteriorating processes of heat resistant steels, and the coarsening law is often described by the Ostwald ripening theories that will be mentioned in section 2.1.

2.1 Ostwald ripening theories

The Ostwald ripening theories, in which the driving force for precipitate coarsening is due solely to the change in interfacial energy accompanied by the change in size distribution of precipitates, have been treated by various investigators.[16–21] When the relevant mass transport is controlled by lattice diffusion, the so-called Lifshitz-Wagner's equation, eq. (1), is applicable.

$$r^3 - r_0^3 = Kt, \tag{1}$$

where r and r_0 are the precipitate radii at time t and $t = 0$, respectively, and K is the coarsening rate constant including lattice diffusivity. The size exponent of the coarsening law is a measure of the corresponding diffusion mechanisms. In practice, the size exponent of 5[18] and 4[19–21] are proposed respectively for pipe diffusion control and grain boundary diffusion or interface diffusion control in stead of 3 for lattice diffusion control.

The classical Ostwald ripening theories, which were proposed originally for single component systems, have been developed to multi-component systems.[22,23] According to Umantsev *et al.*, the rate constant K in eq. (1) is given as below when the chemical composition of precipitates is kept constant during coarsening.

$$K = (64\Gamma/9RT)[(V_m^{PPT})^2/V_m^{matrix}]D_M[X_M^{PPT/matrix}/(X_M^{PPT} - X_M^{matrix})], \tag{2}$$

*Graduate Student, Yokohama National University.

where V_m^{PPT} and V_m^{matrix} are the molar volumes of precipitate and matrix, respectively, Γ is the interfacial energy, D_M is the diffusion coefficient of a component M in the precipitates, $X_M^{PPT/matrix}$ is the molar fraction of a component M in the interface between matrix and the precipitate, X_M^{PPT} and X_M^{matrix} are molar fractions of a component M in precipitate and matrix, respectively. Here assumption will be made that the magnitude of $X_M^{PPT/matrix}$ is approximately equal to that of X_M^{matrix}.

2.2 Particle growth during creep

Since the T91 has a tempered martensitic structure with highly populated dislocations, it is conceivable that the pipe diffusion contributes to the precipitate coarsening along with the lattice diffusion. In the case where the contribution of pipe diffusion is not negligible, the effective diffusivity may be given by eq. (3) in analogy with the case of self-diffusion.[24)]

$$D^* = f_L D_L + f_p D_p, \tag{3}$$

where f_L and f_p are the atomic fractions of atoms participating in lattice and pipe diffusion, D_L and D_P are diffusivities corresponding to lattice and pipe diffusions, respectively. The magnitude of f_L is close to unity and the magnitude of f_p is thus given as;

$$f_p = (n/N)\rho, \tag{4}$$

where n is the number of atoms around a dislocation associated with pipe diffusion, namely n is about 10, and N is the number of atoms per unit area. The magnitude of (n/N) is about $5.8 \times 10^{-19}\,m^2$[25)] and sometimes it is called the cross sectional area of a dislocation pipe, A_p. Since the dislocation density is proportional to the square of applied stress, the effective diffusion coefficient is expressed as below,[26)]

$$D^* \approx D_L[1 + S(\sigma/E)^2(D_P/D_L - 1)], \tag{5}$$

where S is the constant, σ is applied stress, and E is the Young's modulus.

Spigarelli *et al.*[13)] found that the apparent stress dependence of the precipitate coarsening of T91 could not be described properly by eq. (5). In other words, the actual stress dependence of the rate constant was much larger than that expected from eq. (5). For this reason, they exploited the empirical equations in which the apparent activation energy for diffusion was stress dependent. Their equations employed for fitting the experimental results are as below.[13)]

$$\Delta H_C = \Delta H_{OC} + G(T, \sigma). \tag{6}$$

$$G(T, \sigma) = -k(\sigma/E)^p. \tag{7}$$

$$K = K_0 \exp[k(\sigma/E)^p]. \tag{8}$$

$$K_0 = (8D_0\Gamma C_0 V_m^2/9RT)\exp(-\Delta H_{OC}/RT), \tag{9}$$

where ΔH_{OC} is the activation energy of the process that controls the coarsening of the precipitates at zero stress, $G(T, \sigma)$ is a generic temperature and stress dependent parameter, k and p are parameters depending on the type of precipitates, and D_0 is the frequency factor. Spigarelli *et al.*[13)] showed that the magnitude of $[(d^3 - d_0^3)/K]$ was proportional to time, where d and d_0 are diameter of precipitates at t and $t = 0$, respectively. However, the physical significance of these empirical equations is not yet clear.

3. Strain Dependent Diffusivity

3.1 Scavenging effect

Spigarelli *et al.*[13)] showed that the stress dependence of the rate constant is much larger than that expected from eq. (5). Since the increase in stress means the increase in strain rate, it can be viewed that the increase in diffusivity with the increase in stress is due to the increase in diffusivity with increasing strain rate. Actually, the onset of power law breakdown of creep (PLB) is well explained by the increase in diffusivity due to the increase in dislocation density, and also increase in excess vacancies introduced by plastic deformation.[27)] However, the present strain rates are well below the strain rate for PLB. Therefore, another reasoning is required to explain the increase in diffusivity.

Cohen[28)] proposed the criterion to disclose the temperature-strain rate region within which the diffusivity enhancement can be detectable on the experimental basis. The proposed criterion is consistent with many experimental results and it is given by eq. (10).

$$T/T_m \ll 4.9/[2.2 - \log(\text{strain rate})]. \tag{10}$$

Taking 1812 K and 873 K for the melting temperature of T91 and the testing temperature, respectively, it was found that the strain rates which satisfied the above condition was higher than $0.69\,s^{-1}$. This strain rate is extremely higher than the present case. Therefore, the possibility that the enhanced diffusivity due to plastic strain rate can be safely discarded. Thus, an alternative reason must be sought for the apparent stress dependence of diffusivity. One of the other possible candidates is the scavenging effect of dislocation.[29)] Actually, the apparent stress dependence can be viewed as the effect of strain because creep strain at a given time increases with increasing applied stress.

Hereinafter, the effect of strain on precipitate coarsening will be treated. Let us imagine a moving dislocation dragging a solute atmosphere behind it. This is a kind of solute transport by dislocations (the scavenging effect) and the basic concept is presented schematically in Fig. 1, where P is a growing precipitate, lines a and b denote the dislocation positions before and after the movement, and solid and semi-solid circles designate solute atom sites. Since many heat resistant steels usually contain solutes with a relatively large size misfit, a solute atmosphere is formed around a dislocation due to the elastic interaction. When such a

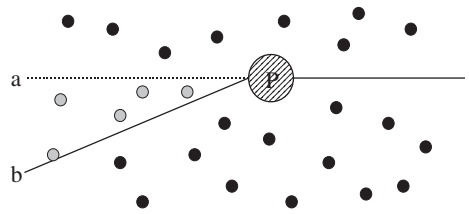

Fig. 1 Schematic illustration of scavenging effect. The dotted line (a) and solid line (b) represent the dislocation lines before and after their motion. The symbol, P represents the growing precipitates.

dislocation encounters a growing precipitate, solute flow is expected to occur from the atmosphere to the growing precipitate along dislocation core because the ratio of D_P/D_L is about 10^3 to 10^4 in the creep regime. This means that once solutes are collected around a moving dislocation, they promote the coarsening of precipitate. In Fig. 1, semi-solid circles represent the sites of solute atoms captured by the moving dislocation.

3.2 Effective area of solute diffusion via dislocation pipe

As Hart showed,[24] the contribution of pipe diffusion to self-diffusivity becomes important when dislocation density is high. In the case of self-diffusion, the cross-section for core diffusion is almost equal to the area of dislocation pipe. However, in the case of solute diffusion, the area related to core diffusion is expected to be different from the area related to self-diffusion. This is because solute diffusivity is enhanced within solute atmosphere due to the interaction between dislocation and a solute atom. Furthermore, as shown in Fig. 1, the solute transport via dislocation core becomes more important when dislocations are moving with solute atmosphere.

The characteristic area related to core diffusion of solutes is different between a stationary dislocation and a moving dislocation. Figure 2(a) is a schematic illustration of the characteristic area for a stationary dislocation, and Fig. 2(b) is that for a moving dislocation. The symbols L and s appearing in Fig. 2 are the effective diameter of the relevant solute atmosphere and the displacement of dislocation, respectively. As shown in Fig. 2, the characteristic diffusion area for a stationary dislocation is $(\pi L^2/4)$ and that for a moving dislocation is the product of L and s. Since the effective area for core diffusion is equivalent to the total area occupied by solutes within the characteristic area, the effective area for the former is $(\pi L^2/4)\overline{C}$ and that for the latter is LsC_0, where $\overline{C}$ is the average solute concentration in a solute atmosphere and C_0 is the average solute concentration in matrix.

Meanwhile, tensile strain is expressed as below;

$$\varepsilon = \phi\rho bs, \tag{11}$$

where ϕ is a conversion factor from shear strain to tensile strain of about 0.5, b is the magnitude of Burgers vector, ρ is the dislocation density. Using eq. (11), LsC_0 is expressed by $(2LC_0\varepsilon/\rho b)$. Thus, the effective diffusivities of solutes for stationary and moving dislocations are given by eqs. (12) and (13), respectively.

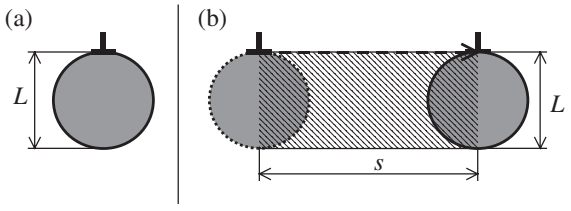

Fig. 2 Schematic illustration of the characteristic area related to core diffusion of solute. The shaded area below a static dislocation in (a) designates the characteristic area, and the hatched area in (b) designates the increment of the characteristic area for the movement of dislocation.

$$D_{\text{eff}} = D_L + (\pi L^2\overline{C}/4)\rho D_P. \tag{12}$$

$$D^*_{\text{eff}} = D_L + (2LC_0\varepsilon/b)D_P. \tag{13}$$

As eq. (13) shows the effective diffusivity for gauge part is expected to change linearly with plastic strain.

4. Result of Analysis and Discussion

4.1 Source of analyzed data

In the previous work two of the present authors (Spigarelli and Evangelista) have conducted creep tests on T91 and examined the coarsening law of precipitates. The chemical composition of the creep specimen was Fe–0.091C–0.40Si–0.46Mn–8.76Cr–0.94Mo–0.11Ni–0.035Al–0.064N–0.07Nb–0.19V in mass %. Normalizing and tempering subjected to specimens were at 1323 K for 900 s and at 1023 K for 3600 s, respectively. Short term constant load creep tests were performed at 848, 873, 898 and 923 K under stresses ranging from 85 to 280 MPa. Specimens were tested to failure except for a series of interrupted test conducted at 873 K and 848 K. Sample elongation was measured using linear variable transducers.

The results of measured average particle size are listed in Table 1. In a Mod.9Cr–1Mo steel (T91), there are two types of precipitates, $M_{23}C_6$ and MX. These diameters are represented by d_I and d_{II}, respectively. Initial size of these particles were 70 nm and 20 nm, respectively. In Table 1 the magnitude of strain is also shown although some of the strain values are estimated from the constitutive equations[30] using corresponding experimental conditions.

4.2 Growth controlling diffusion species

Usually precipitates in heat resistant steels are composed of multi-components. It is, therefore, quite natural to view that more than two diffusion species take part in the coarsening process of precipitates. In eq. (2), assumption will be made that $X_M^{\text{PPT/matrix}}$ is equal to X_M^{matrix}. Since Γ, V_m^{PPT} and V_m^{matrix} are all material constants, and T is a constant given by the experimental condition, the magnitude of K controlling the coarsening rate is determined by a diffusion species which minimize the magnitude of $D_M[X_M^{\text{PPT/matrix}}/(X_M^{\text{PPT}} - X_M^{\text{matrix}})]$ in eq. (2). Kadoya *et al.*[31] have shown that the chemical composition of $M_{23}C_6$ is 9.0 at%Fe–9.7%Mo–60.5%Cr–207%C at 873 K and it is almost constant during creep of Mo or W bearing 12Cr steels. Using this fact that the chemical composition of precipitates remains constant during coarsening, the $D_M[X_M^{\text{PPT/matrix}}/(X_M^{\text{PPT}} - X_M^{\text{matrix}})]$ values for $M_{23}C_6$ were calculated to be 1.33×10^{-19} m^2/s for Cr and 1.52×10^{-21} m^2/s for Mo at 873 K. Based on these results, the diffusion species controlling the growth rate of $M_{23}C_6$ is expected to be the diffusion of Mo atoms.

On the other hand, it is rather difficult to identify the diffusion species controlling the growth rate of MX precipitates because the knowledge on the concentration of Nb and V in matrix, which are the main components of MX precipitate particles, is limited. Furthermore, it is not clear whether or not the composition of MX is kept constant during the course of creep. In the present paper, the analysis will be

Table 1 Results of particle size in T91 after creep testing: dimensions of precipitates in steel of similar composition after different heat treatment[12] and the data on the previous work[13] are included.

Part of specimen	Stress, σ/MPa	Temperature, T/K	Creep time, $t/10^6$ s	Strain, ε	Mean diameter of $M_{23}C_6$ type precipitates, $d_I/10^{-8}$ m	Mean diameter of MX type precipitates, $d_{II}/10^{-8}$ m
gauge	85	923	2.66	0.26	15.6	2.7
gauge	175	873	1.03	0.06	9.5	3.2
gauge	105	873	15.7	0.015	10.5	4.0
gauge	130	873	1.81	0.012	7.0	2.2
gauge	105	873	119	0.0087	19.5	7.3
gauge	130	873	9.87	0.03	11.4	3.3
grip	30	873	15.7	0	9.7	2.3
grip	30	873	119	0	14.0	5.1
gauge	215	848	1.52	0.15	8.5	2.2
gauge	185	848	13.2	0.12	11.5	3.2
gauge	130	848	13.7	0.0125	7.6	2.4
gauge	185	848	1.99	0.011	7.2	2.1
gauge	130	848	5.78	0.0065	7.7	2.4

made on the assumption that the growth rate of precipitate MX is governed by the diffusion of V atoms. This is because the concentration of Nb in matrix is expected to be almost zero in service states. Actually, the result of the ThermoCalc shows that the concentration of Nb in matrix is almost zero at tempering temperature. Thus, there is no plausible reason to assume that Nb atoms take part in the important role in coarsening of MX during creep. On the other hand, the main component of MX precipitates, V (42.7 at%V–8.9%Nb–48.3%N–0.1%C at 873 K) atoms dose not precipitate during normalizing and precipitates during tempering as MX. Therefore, it is expected that some fraction of V remains in matrix after tempering, and it affects the rate of growth of MX during creep.

4.3 Numerical estimate of L value

The size misfit parameters of Cr, Mo, V and Nb in T91 are 0.0143, 0.0843, 0.0338 and 0.0610, respectively.[32] Because of these size misfits, solute atmosphere is formed around dislocations. As Cottrell assumed, an assumption will be made that the solute concentration around a dislocation is expressed by a Maxwellian distribution as below;[33]

$$C(x) = C_0 \exp(W/kT), \tag{14}$$

where C_0 is the average solute concentration in matrix and $C(x)$ is the solute concentration at a distance x apart from the dislocation, and W is the elastic interaction energy between a solute and the dislocation.

The elastic interaction energy, W is given as;[33]

$$W = A(\sin\theta/x), \tag{15}$$

where A is a constant given as below;

$$A = (4/3)[(1+\nu)/(1-\nu)]Gb\eta R_0^3, \tag{16}$$

where ν is a Poisson's ratio of 0.345, $G = 6.60 \times 10^4$ MPa, R_0 is the radius of a solvent atom of the magnitude of 1.24×10^{-10} m, and η is the size misfit parameter. For simplicity, taking $(\sin\theta)$ being equal to unity, Cottrell defined L as a distance at which $C(L)/C_0$ being equal to e.[33] However, this magnitude of L seems too small. So in the present study, the effective diameter L was defined as a distance at which $C(L)/C_0$ is equal to 1.5 in stead of e. This value is based on the result of numerical simulation concerning a simple binary system. The preliminarily conducted numerical simulation showed that L corresponding to $C(L)/C_0$ being equal to 1.5 is independent of dislocation velocity as far as dislocation is moving in a Newtonian viscous manner. However, it decreases suddenly when the linear relation between dragging stress and dislocation velocity breaks down. The procedure for the numerical simulation was shown in elsewhere.[34,35] The magnitude of L is thus expressed as below;

$$L = (4/3)[(1+\nu)/(1-\nu)](Gb\eta R_0^3/kT \ln 1.5). \tag{17}$$

Using eq. (17), the magnitudes of L for Mo and V at 873 K are estimated to be about $5.6b$ and $2.2b$, respectively.

4.4 Diffusivity compensated growth rate

Based on the model so far mentioned, the effective solute diffusivities were calculated, and an example of the calculated result is given in Table 2. The effective diffusivities given in Table 2 correspond to 0.87% strain obtained from the creep test at 873 K for 1.19×10^8 s under an initial stress of 105 MPa. Stress at grip part was estimated to be 30 MPa. In the present calculation, the average solute concentration within the atmosphere of diameter L, $\overline{C}(L)$ was assumed to be equal to $C(L)$, *i.e.* $\overline{C}(L) = 1.5C_0$. The material constants necessary for the calculation are listed in Table 3, and solubilities of the main solutes in matrix are given in Table 4. As Table 2 shows, the magnitude of $(\pi L^2\overline{C}/4)\rho D_P$ corresponding to the grip part is much smaller than the magnitude of D_L. Therefore, even in the case of T91 with high dislocation density, the contribution of core diffusion to precipitate coarsening is quite small so far as dislocations are at rest. To the contrary, the magnitude $(2LC_0\varepsilon/b)D_P$ becomes comparable to D_L when dislocations are moving with solute atmospheres. In Figs. 3 and 4, the magnitude of $(d^3 - d_o^3)$ is plotted against time on a double logarithmic scale for $M_{23}C_6$

Table 2 An example of calculated effective diffusivities*.

Type of precipitates	Part of specimen	Lattice diffusivity, D_L/m^2s^{-1}	Increment of solute diffusivity due to the presence of dislocations, $(\pi L^2\overline{C}/4)\rho D_P/m^2s^{-1}$	Increment of solute diffusivity due to moving dislocations, $(2LC_0\varepsilon/b)D_P/m^2s^{-1}$	Effective diffusivity, D_{eff}/m^2s^{-1}
$M_{23}C_6$	grip	4.1×10^{-20}	7.8×10^{-23}	—	4.1×10^{-20}
	gauge		—	5.1×10^{-20}	9.1×10^{-20}
MX	grip	3.9×10^{-21}	1.0×10^{-24}	—	4.0×10^{-21}
	gauge		—	1.6×10^{-21}	5.6×10^{-21}

*The effective diffusivities given here correspond to 0.87% strain tested at 873 K for 1.19×10^8 s under an initial stress of 105 MPa. Stress at grip part was estimated to be 30 MPa.

Table 3 Material constants used for calculation of effective diffusivity.

Lattice diffusivity, $D_L = D_{0L}\exp(-Q_L/RT)$	Cr in Fe	$D_{0L}(m^2/s) = 8.52 \times 10^{-4}$ $Q_L(kJ/mol) = 251$	Ref. 36)
	Mo in Fe	$D_{0L}(m^2/s) = 4.6 \times 10^{-3}$ $Q_L(kJ/mol) = 285$	Ref. 37)
	V in Fe	$D_{0L}(m^2/s) = 0.25 \times 10^{-4}$ $Q_L(kJ/mol) = 264$	Ref. 38)
	Nb in Fe	$D_{0L}(m^2/s) = 5.30 \times 10^{-2}$ $Q_L(kJ/mol) = 344$	Ref. 36)
Pipe diffusivity, $A_P D_P = A_P D_{0P}\exp(-0.6Q_L/RT)$	$A_P(m^2) = 5.80 \times 10^{-19}$ $A_P D_{0P}(m^4/s) = 1.0 \times 10^{-24}$		Ref. 25)
Burgers vector, b/m	2.48×10^{-10}		
Shear modulus, G/MPa	$-48T(/K)+103572$		Ref. 5)
Dislocation density within lath martensite, ρ/m^{-2}	$0.3075(\sigma/G)^2(1/b)^2$		Ref. 5)

Table 4 Solubility limits in atomic fraction at various temperatures.

	923 K	873 K	848 K
Cr	0.083	0.082	0.082
Mo	0.0036	0.0035	0.0035
V	0.0001	0.00005	0.00005
Nb	0.00003	0.00003	0.00003

and MX precipitates. As these figures show, the coarsening rate of gauge part is larger than that of grip part although some scattering of data exists. Figures 5 and 6 show the relationship between $(d^3 - d_o^3)/D_{eff}$ and time plotted on a double logarithmic scale. It is seen that the magnitude of $(d^3 - d_o^3)/D_{eff}$ changes linearly with time, and the data on both grip and gauge parts fall around the normalized line. Because of the lack of exact data on solute concentration of matrix and dislocation density, which are all necessary for the calculation of effective diffusivities, some ambiguities remain on the magnitude of effective diffusivity. However, the conclusion can be drawn that the scavenging effect of dislocation becomes important when creep strain is large. Two of the present authors (Nakajima and Endo) have ascertained from the experimental works on Al–Cu alloys and a magnesium alloy of AZ80 that the precipitate coarsening during creep is enhanced by creep strain.[39] These facts also reinforce the assertion that plastic strain promotes the solute diffusivity during creep.

4.5 Size exponent of coarsening law

As mentioned in section 2, the size exponent of coarsening law is a good measure to identify the relevant rate controlling mechanism. However, actual coarsening process of T91 is not so simple because it contains highly populated dislocations favorable for core diffusion and many of $M_{23}C_6$ are liable to precipitate on subgrain boundaries which are favorable for boundary diffusion. For this reason, two or three other mechanisms are expected to occur simultaneously along with solute transport by lattice diffusion. Besides these, Hald and Korcakova[40] pointed out the importance of the change of interface during aging, *i.e.*, from partially coherent to incoherent interface, which inevitably affect the rate constant in eq. (2) through interfacial energy.

Kadoya *et al.*[31] have studied the coarsening of $M_{23}C_6$ and MX precipitates during creep of Mo or W bearing 12Cr steels. They reported that the coarsening rate of $M_{23}C_6$ particles, found on subgrain boundaries, were consistent with the third power dependence of particle radius with an activation energy similar to lattice diffusion, while that of MX particles, which lay on the subgrain interior dislocation lines, were better explained by core diffusion with the fifth power dependence on particle radius and an activation energy approximately half of the bulk diffusion. Kimura *et al.*[41] have studied recently the coarsening of $M_{23}C_6$ and MX during creep of T91. Their paper makes no mention of the size exponent. However, their figure shows implicitly that the

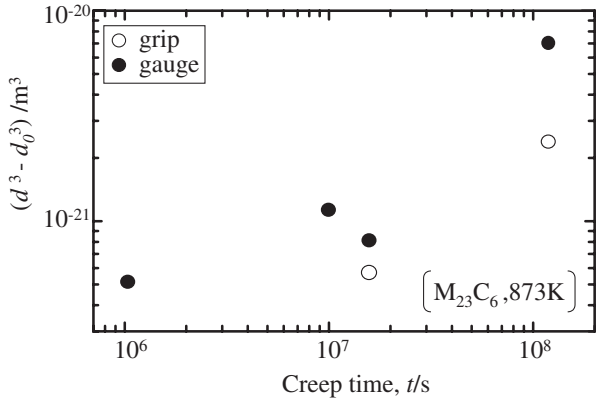

Fig. 3 Relation between $(d^3 - d_0^3)$ and creep time for $M_{23}C_6$ type precipitates.

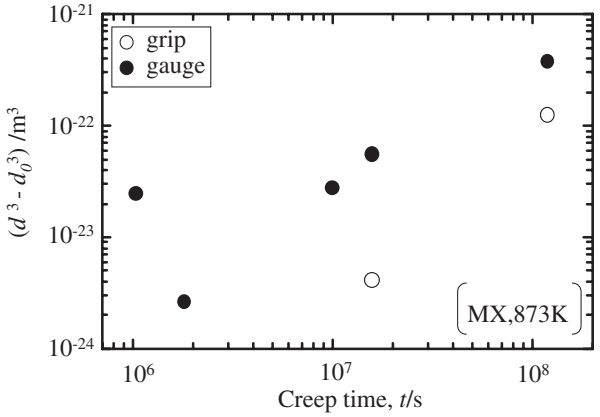

Fig. 4 Relation between $(d^3 - d_0^3)$ and creep time for MX type precipitates.

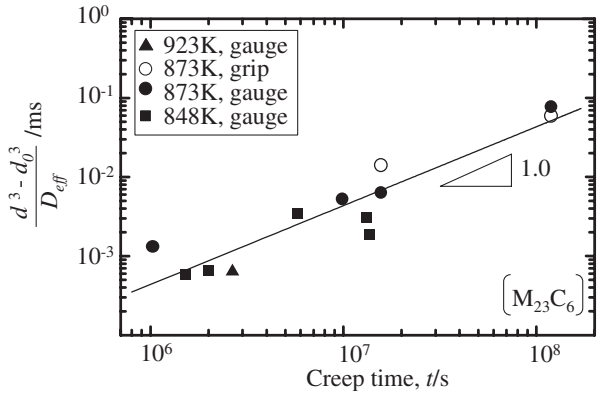

Fig. 5 Relation between $(d^3 - d_0^3)$ for $M_{23}C_6$ type precipitates compensated by effective diffusivity and creep time.

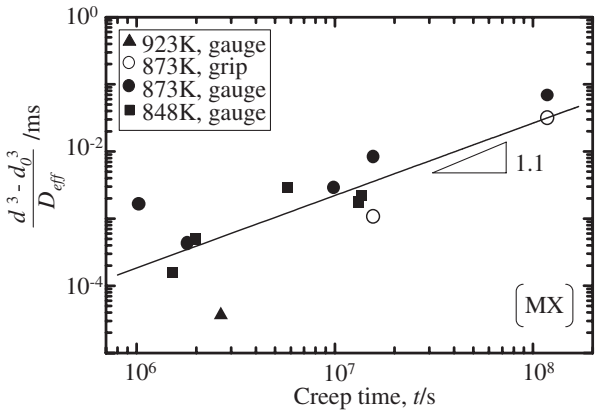

Fig. 6 Relation between $(d^3 - d_0^3)$ for MX type precipitates compensated by effective diffusivity and creep time.

size exponent of MX is smaller than that of $M_{23}C_6$. In the present analysis, the possibility of the fifth power dependence on particle radius was actually examined. However, it was ascertained that the size exponent of 3 gives better fit even for MX particles. At present time it is not yet clear why such a discrepancy occurs. However, the difference in tempering and testing temperatures should be noted. In practice, the tempering temperature of 12Cr steels was about 823 to 923 K while that of T91 was about 1323 K and the testing temperature of the former was at tempering temperature, while that of T91 was at 873 K. In addition, for the dislocation-aided coarsening to become dominant, Dunlop and Honeycombe[42] pointed out that the precipitates must be coherent or semi-coherent with matrix and the dislocation density participating in growth must be greater than some minimum value. In order to make clear the reason for the inconsistency, further study is necessary.

5. Summary

Data on the precipitate coarsening during creep of a T91 steel, which was dependent not only on time and temperature but also on stress apparently, were reanalyzed. In the present study, the effective diffusivity dependent on creep strain was calculated on the assumption that the dislocation movement with solute atmosphere contributes to solute transport during coarsening and the Ostwald ripening as a result. The volume change accompanied by the Ostwald ripening, which was compensated by effective diffusivity was examined both on grip and gauge parts. The volume change compensated by the effective diffusivity of gauge part of creep specimens was consistent with that in grip parts notwithstanding the coarsening rate in gauge part was apparently higher than those in grip parts. This strongly suggests that the motion of dislocations with solute atmosphere enhances the precipitate coarsening during creep.

REFERENCES

1) V. Sklenicka, K. Kucharova, D. Dulouhy and J. Krejci: *Materials for advanced power engineering*, ed. by D. Coutsouradis *et al.*, (Kluwer, Dordrecht, 1994) pp. 435–444.
2) V. Foldyna, A. Jakobova, A. Gemperle and R. Riman: *Creep and fractures of engineering materials and structures*, ed. by B. Wilshire and R. W. Evans, (Inst. of Met., UK, 1990) pp. 507–516.
3) K. Sawada, K. Maruyama, Y. Hasegawa and T. Muraki: *Creep and Fracture of Engineering Materials and Structures*, ed. by T. Sakuma and K. Yagi, (Trans. Tech Publications, Key Engineering Materials, vols. **171–174** (2000) 109–114).
4) K. Sawada, M. Takeda, K. Maruyama, R. Komine and Y. Nagae: Tetsu to Hagane **84** (1998) 40–45.
5) K. Sawada, K. Maruyama, R. Komine and Y. Nagae: Tetsu to Hagane **83** (1997) 54–59.

6) K. Suzuki, S. Kumai, H. Kushima, K. Kimura and F. Abe: Tetsu to Hagane **86** (2000) 52–59.
7) T. Endo, F. Masuyama and K.-S. Park: Tetsu to Hagane **88** (2002) 526–533.
8) K.-S. Park, F. Masuyama and T. Endo: J. Japan Inst. Metals **63** (1999) 597–600.
9) H. Kushima, K. Kimura and F. Abe: Tetsu to Hagane **85** (1999) 57–63.
10) T. Nishizawa, I. Ohmura and K. Ishida: Mater. Trans., JIM **38** (1977) 950–956.
11) S. Straub, T. Hennige, P. Polsik and W. Blum: Steel Res. **66** (1995) 394–401.
12) S. Straub, P. Polsik, W. Besigk, W. Blum, H. Konig and K. H. Mayer: Steel Res. **66** (1995) 402–408.
13) S. Spigarelli, E. Cerri, P. Bianchi and E. Evangelista: Mater. Sci. Tech. **15** (1999) 1433–1440.
14) M. Taneike, M. Kondo and T. Morimoto: ISIJ Int. **41** (2001) S111–S115.
15) M. Hättestrand and H. O. Andrén: Acta Mater. **49** (2001) 2123–2128.
16) C. Wagner: Z. Elecktrochem. **65** (1961) 581–591.
17) I. M. Lifshitz and V. V. Slyozov: J. Phys. Chem. Solids **19** (1961) 35–50.
18) M. Kreye: Z. Metallk. **61** (1970) 108–112.
19) M. H. Speight: Acta Metall. **16** (1968) 133–135.
20) A. J. Ardel: Acta Metall. **20** (1972) 601–609.
21) A. J. Ardel: Acta Mettall. **15** (1967) 1772–1775.
22) M. Y. Wei, T. Sakuma and T. Nishizawa: Tetsu to Hagane **65** (1980) S1178.
23) A. Umantsev and G. B. Olson: Scr. Metall. Mater. **30** (1993) 1135–1140.
24) E. W. Hart: Acta Metall. **5** (1957) 597.
25) H. J. Frost and M. F. Ashby: *Deformation Mechanism Maps*, (Pergamon Press, UK, 1982) pp. 30–42.
26) O. D. Sherby and C. M. Young: *Proc. J. E. Dorn Symp. on Rate Processes in Plastic Deformation of Materials*, ed by J. C. M. Li and A. K. Mukherjee, (ASM., OH. 1976) pp. 497–541.
27) P. E. Armstrong, W. V. Green, O. D. Sherby and E. G. Zukas: Acta Metall. **21** (1973) 1319–1326.
28) M. Cohen: Bull. Japan Inst. Metals **9** (1970) 271–278.
29) A. Mortlock: Acta Metall. **8** (1960) 132–134.
30) K.-S. Park, F. Masuyama and T. Endo: ISIJ Int. **41** (2001) Supple. S86–S90.
31) Y. Kadoya, B. F. Dyson and M. McLean: *Materials for Advanced Power Engineering*, ed. by J. Lecomte-Beckers *et al.*, (Forshungszentrum Jülich GmbH, Jülich, 1998) pp. 593–693.
32) A. H. King: Mater. Sci. Eng. **1** (1966) 79–90.
33) A. H. Cottrell: *Dislocations and Plastic Flow in Crystals*, (Oxford Press, UK. 1953) pp. 133–139.
34) T. Endo, M. Tasaki, M. Kubo and T. Shimada: Trans. JIM **23** (1982) 665–673.
35) T. Endo, T. Shimada and T. G. Langdon: *Proc. of ICSMA 7*, ed. by H. J. McQueen, J.-P. Bailon, J. I. Dickson, J. J. Jonas and M. G. Akben, 1985, pp. 794–796.
36) A. W. Bowen and G. M. Leak: Metall. Trans. **5** (1970) 1695–1700.
37) Kinzoku deta bukku (in Japanese): Maruzen, p. 25.
38) B. Sparke, D. W. James and G. M. Leak: J. Iron and Steel Inst. **203** (1965) 152–153.
39) N. Nakajima, M. Takeda and T. Endo: unpublished.
40) J. Hald and L. Korcakova: *28. MPA-Seminar, Safety and Reliability in Energy Technology*, (MPA Sttugart Univ. Germany, 2002) vol. **2**, pp. 54.1–54.19.
41) K. Kimura, K. Suzuki, H. Kushima and F. Abe: *10th joint int. conf. on Creep and Fracture of Engineering Materials and Structures*, Part Creep Resistant metallic Materials, (Vitkovice-Research and Development, Cz. 2001) pp. 186–195.
42) G. L. Dunlop and R. W. K. Honeycombe: Philos. Mag. **32** (1975) 61–72.